Direct imaging of the depletion region of an InP $p-n$ junction under bias using scanning voltage microscopy

D. Ban[a] and E. H. Sargent
Department of Electrical and Computer Engineering, University of Toronto, 10 King's College Road, Toronto, M5S 3G4, Canada

St. J. Dixon-Warren,[b] I. Calder, A. J. SpringThorpe,[a] R. Dworschak, G. Este, and J. K. White
Nortel Networks Optical Components, 3500 Carling Avenue, Ottawa, Ontario, K2H 8E9, Canada

(Received 2 July 2002; accepted 21 October 2002)

We directly image an InP $p-n$ junction depletion region under both forward and reverse bias using scanning voltage microscopy (SVM), a scanning probe microscopy (SPM) technique. The SVM results are compared to those obtained with scanning spreading resistance microscopy (SSRM) measurements under zero bias on the same sample. The SVM and SSRM data are shown to agree with the results of semiclassical calculations. The physical basis of the SVM measurement process is also discussed, and we show that the measured voltage is determined by the changes in the electrostatic potential and the carrier concentration at the SVM tip with and without the applied bias.
© *2002 American Institute of Physics.* [DOI: 10.1063/1.1528277]

Imaging the position and width of $p-n$ junction depletion regions in semiconductor materials is of fundamental importance to understanding device physics. Electron beam induced current (EBIC) techniques have been used for many years for this purpose.[1,2] Recently, a variety of scanning probe microscopy techniques have been developed[3,4] that allow direct imaging of semiconductor structures, including $p-n$ junctions, with nanometer spatial resolution. The techniques include scanning spreading resistance microscopy (SSRM)[5,6] and scanning capacitance microscopy,[7] which have been used for two-dimensional dopant profiling of semiconductor devices. The quantitative capabilities of these techniques have been demonstrated on unbiased Si-based structures[8] and InP-based structures.[9,10] Scanning voltage microscopy (SVM)[11] is a technique that delineates, in two dimensions, the voltage on the cross section of semiconductor devices. It sheds light on the electrical characteristics of the devices under a variety of operating conditions, providing a direct view into the behavior of operating semiconductor devices. It provides information that is not available with electron beam techniques such as EBIC.

Trenkler and coworkers demonstrated the application of SVM, which they called *nanopotentiometry*, on Si-based metal–oxide–semiconductor field-effect-transistor devices and interpreted their results terms of the average of electron and hole quasi-Fermi-levels.[12] We also assume an understanding that the SVM measurement can rely on near-equilibrium equations. We derive a relation for the measured SVM signal that involves the single-particle electrostatic potential, used in the Schrödinger equation, and the local carrier concentration. This relationship gives physical insight into the SVM measurement process, although it does not adequately account for many-body effects.[13] It is therefore not quantitatively exact in the treatment of far-from-equilibrium regions of a device, such as the active region of a laser biased above lasing threshold. It is worth noting that in 1952, Pearson *et al.* reported voltage measurements with a tungsten probe on the cross section of a diffused germanium $p-n$ junction with approximately 2 μm spatial resolution.[14]

In this letter, we report the application of SVM to InP-based $p-n$ junction: the foundational functional unit of electronic and optoelectronic devices. We begin by reporting SSRM results that delineate the buried transverse cross section of the $p-n$ junction sample. We then report one-dimensional voltage profiles across the junction with high spatial resolution under different bias voltages. We directly observe the variation of the depletion region on nanometer scale as the bias voltage increases. We compare our results with semi-classical $p-n$ junction theory.

SVM was performed using a commercial atomic force microscope (AFM) (Digital Instruments, Dimension 3100). The local voltage was measured by an ultrahigh-impedance voltmeter (Keithley 6517 A) connected to a conductive AFM tip. Boron-doped diamond-coated cantilever tips (DDESP, Digital Instruments) were used in contact mode on the cleaved cross section of the $p-n$ junction. The contact force was set such that the tip mechanically penetrated the native oxide layer at the sample surface to establish a good electrical contact. We obtained a spatial resolution on the order of the radius of the AFM tip ($\sim$20 nm). Further details of experimental setup are provided in Ref. 15. The SSRM measurements were also performed on the same instrument with the same tips, by using appropriate SSRM applications module.

The $p-n$ junction sample grown by molecular beam epitaxy consisted of two 500-nm-thick InP layers. The two layers were Be- (for p-type) and Si-doped (for n-type), respectively, both with the nominal doping concentration of 1×10^{18} cm^{-3}. A heavily p-doped 200 nm InGaAs layer was grown at the top surface of the $p-n$ junction for better ohmic contact. A simple cleave was taken to expose the cross sec-

[a]Also at: Institute for Microstructural Sciences, National Research Council, 1200 Montreal Road, Ottawa, Ontario, Canada K1A OR6.
[b]Author to whom correspondence should be addressed; electronic mail: stj.dixon.warren@utoronto.ca

0003-6951/2002/81(26)/5057/3/$19.00 © 2002 American Institute of Physics
Downloaded 20 Dec 2003 to 128.100.138.68. Redistribution subject to AIP license or copyright, see http://ojps.aip.org/aplo/aplcr.jsp

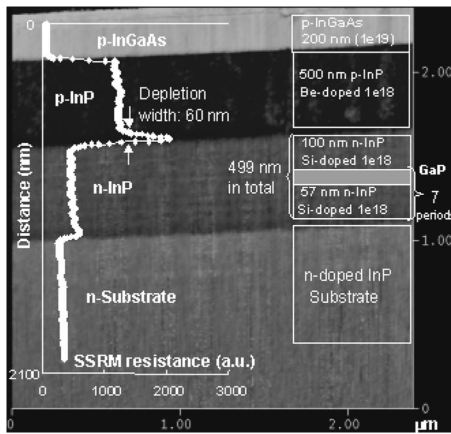

FIG. 1. An SSRM image of the $p-n$ junction sample. The scan rate is 0.25 Hz and tip dc bias is 1.0 V. The ultrathin (0.37 nm) GaP mark layers, as shown in the inset, are resolved in the image. The cross-sectional SSRM resistance curve overlaid on the image shows the depletion width of the $p-n$ junction at equilibrium is approximately 60 nm.

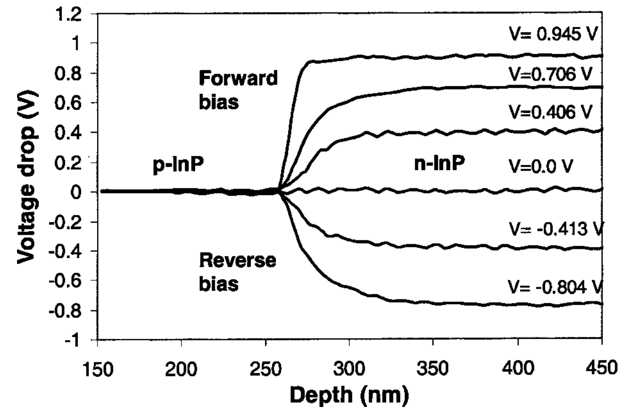

FIG. 2. Cross-sectional voltage drop across then $p-n$ junction under forward and reverse biases. Voltage falls essentially within the depletion region of the $p-n$ junction. The voltage drop curves show that the depletion region shrinks as the applied voltage changes from reverse to forward bias.

tion of the $p-n$ junction. Colloidal silver paint was used to provide electrical contact to the p and n sides of the sample. The sample bar was then mounted with the cleaved edge facing up in a metal clamp that provided electrical contact to the p and n side of the sample. The current–voltage characteristics of the samples were measured before, during, and after the SVM experiment to confirm diode behavior. Stable electrical device characteristics were obtained. AFM images of the sample surface, obtained simultaneously with the SSRM and SVM data, showed no perceptible topographic features.

SSRM was first deployed to examine the cross section of the $p-n$ junction structure. Figure 1 shows an SSRM image obtained on the freshly-cleaved facet of the $p-n$ junction. The n^+ substrate is the band at the bottom. Topmost is the heavily p-doped InGaAs layer. The p- and n-doped InP layers are clearly resolved in the SSRM image. The 0.37-nm-thick GaP marker layers within the n-doped InP layer, as shown in the inset of the schematic structure of the sample, can be resolved in the image, attesting to the high spatial resolution of this technique. The cross-sectional SSRM resistance curve overlaid on the image shows that the depletion width of the $p-n$ junction is around 60 nm. The impact of the GaP marker layers on the electrical characteristics of the $p-n$ junction is expected to be negligible since they are ultrathin and far enough away from the junction depletion region. The SSRM resistance of p-InP is higher than that of n-InP because hole mobility is lower than electron mobility.

SVM measurements were then performed on the cross section of the $p-n$ junction under forward and reverse bias. Figure 2 shows the SVM profiles across the $p-n$ junction under various bias voltages. As the applied voltage changes from reverse to forward, the voltage drop of the n-InP layer (reference to p-contact) increases correspondingly, and the transition region from p- to n-side shrinks, reflecting the change of the depletion region (high-resistive) of the $p-n$ junction. The measured SVM results reveal the applied voltage falls essentially over the depletion region of the $p-n$ junction, as expected from the semiclassical theory.[16]

A voltmeter measures the difference in electrochemical potential between the two contact points on the sample.[17] The electrochemical potential is a thermodynamic quantity, and is not identical to the Fermi level commonly used in semiclassical description of semiconductor device physics. The measured voltage V_{measd} in SVM is given by

$$V_{\text{measd}}=\frac{\mu_e(x)-\mu_e(ref)}{e}, \tag{1}$$

where e is electron charge and $\mu_e(x)$ and $\mu_e(ref)$ are the electrochemical potentials of the tip contact point at an arbitrary position x and a reference point, respectively. At equilibrium the electrochemical potential μ_e remains constant throughout the $p-n$ junction and the voltmeter measures zero voltage drop.

In the presence of an electrostatic field the electrochemical potential $\mu_e(x)$ is given by[18]

$$\mu_e(x)=kT\ln c(x)V_q+q\phi(x), \tag{2}$$

where $c(x)$ is the carrier concentration at x, k is the Boltzmann constant, and T is the temperature. $\phi(x)$ is the single particle electrostatic potential and $V_q=(2\pi^{\|2}/m^*kT)^{3/2}/2$ is the quantum volume which is equal to the inverse of the density of states. Equation (2) is applicable at low-to-moderate carrier concentrations (10^{18} cm^{-3} or less) in semiconductor electronic and optoelectronic devices. Equation (2) shows a higher carrier concentration corresponds to a higher chemical potential.

When a bias voltage is applied to the sample, Eq. (2) should still hold, provided the deviation from equilibrium is not too large. We then obtain the measured voltage

$$V_{\text{measd}}=\phi_b(x)-\phi_0(x)-\frac{kT}{e}\ln\frac{c_b(x)}{c_0(x)}, \tag{3}$$

where subscript b is for nonzero applied bias (nonequilibrium), and subscript *0* is for zero applied bias (equilibrium). Thus, the measured voltage reflects the change of both electrostatic potential and local carrier concentration upon the application of a bias. Since $kT/e=0.026$ V at room temperature is small, the second term in Eq. (3) will only be important for large deviation in the carrier concentration from the equilibrium value. In regions in which the carrier concentra-

Downloaded 20 Dec 2003 to 128.100.138.68. Redistribution subject to AIP license or copyright, see http://ojps.aip.org/aplo/aplcr.jsp

tion does not change significantly upon the application of external bias, then the concentration-dependent term can be neglected, giving

$$V_{\mathrm{measd}}=\phi_b(x)-\phi_0(x). \tag{4}$$

In this case, the measured voltage is simply the difference between the electrostatic potential under bias and the built-in electrostatic potential with zero bias. Equation (4) is expected to apply to majority carrier regions far from the junction, where the carrier concentration does not change with bias. We derived this equation from simple contact potential arguments in a previous paper.[15] A full theory of SVM would require detailed understanding of carrier transport across the tip–sample surface contact.

We use the thermodynamically defined electrochemical potential instead of the Fermi level in deriving Eq. (3), because the electrochemical difference is the macroscopic quantity actually measured by our voltmeter, while the Fermi level is only strictly defined at equilibrium.

The semiclassical model for the $p-n$ junction predicts the appearance of a depletion layer at the $p-n$ junction and allows the calculation of its width as a function of applied bias. The width of the depletion region at equilibrium is given by[19]

$$W_0=\left[\frac{2\varepsilon_r\varepsilon_0 kT}{q^2}\ln\left(\frac{N_aN_d}{n_i^2}\right)\left(\frac{1}{N_a}+\frac{1}{N_d}\right)\right]^{1/2}. \tag{5}$$

The relative permittivity ε_r of InP is 12.56; the doping concentrations of the $p-n$ junction treated herein are $N_a=1.0\times10^{18}\ \mathrm{cm}^{-3}$ and $N_d=1.0\times10^{18}\ \mathrm{cm}^{-3}$; and for InP at 300 K, $n_i=1.2\times10^{8}\ \mathrm{cm}^{-3}$. The depletion region width of the $p-n$ junction at equilibrium is calculated to be $W_0=57$ nm. This agrees well with our measured result of 60 nm from SSRM.

The model gives the depletion width (W) as a function of applied bias (V),

$$W(V)=W_0\left[1-\frac{V}{V_{\mathrm{bi}}}\right]^{1/2}, \tag{6}$$

where W_0 is defined as Eq. (5) and V_{bi} is the built-in voltage across the $p-n$ junction. By taking the derivative of the voltage curves in Fig. 2, one can obtain the transition width in which the voltage changes from zero to applied bias. The measured transition width as a function of bias and calculated depletion width using Eq. (6) under forward and reverse biases are shown in Fig. 3. Excellent agreement is obtained between the experimental and the theoretical results. The measured accumulative voltage drops from p to n sides at each bias voltage are also shown in Fig. 3, and a linear relationship is obtained, confirming that our SVM probe was measuring the voltage difference between the SVM tip contact point and the reference point in the circuit.

Scanning voltage microscopy was used to profile the voltage distribution across the InP $p-n$ junction structure under forward and reverse biases. The variation of depletion width with the application of external bias was observed with nanometer resolution. The voltage measured in SVM is the difference between the electrostatic potential under bias and the built-in electrostatic potential at equilibrium, plus a carrier concentration dependent term that has to be taken into account if the carrier concentration changes significantly from its equilibrium state.

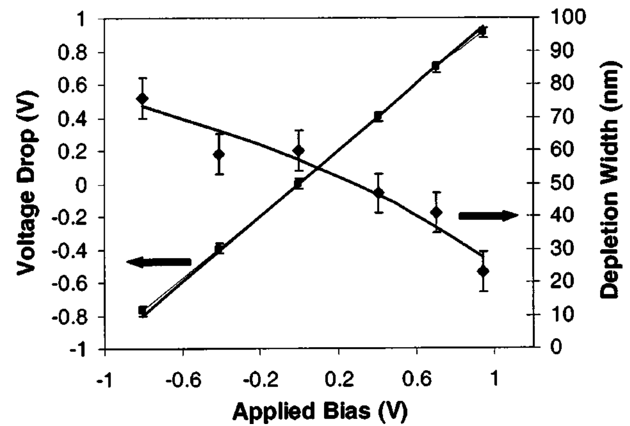

FIG. 3. Measured (discrete diamond) and calculated (solid line) depletion width of the $p-n$ junction under different bias voltages. The measured accumulative voltage drop (discrete square) from p to n side agrees well with the externally applied bias (solid line).

The authors would like to thank Gerry Smith at Nortel Networks, Genlin Tan at Lightcross, Mingwei Xu at IMEC, and Matthew Lefevre at DI for valuable discussions and technical help.

[1] G. S. Fritz, F. E. Prins, and D. P. Kern, Microelectron. Eng. **57–58**, 199 (2001).
[2] T. Koyama, M. Umeno, K. Sonoda, J. Komori, and Y. Mashiko, Microelectron. Reliab. **41**, 1243 (2001).
[3] P. De Wolf, R. Stephenson, T. Trenkler, T. Clarysse, T. Hantschel, and W. Vandervorst, J. Vac. Sci. Technol. B **18**, 361 (2000).
[4] D. Ban, E. H. Sargent, St. J. Dixon-Warren, T. Grevatt, G. Knight, G. Pakulski, A. J. SpringThorpe, R. Streater, and J. K. White, J. Vac. Sci. Technol. B **20**, 2126 (2001).
[5] C. Shafai, D. J. Thomson, M. Simard-Normandin, G. Mattiussi, and P. J. Scanlon, Appl. Phys. Lett. **64**, 342 (1994).
[6] P. De Wolf, J. Snauwaert, L. Hellemans, T. Clarysse, W. Vandervorst, M. D'Olieslaeger, and D. Quaeyhaegens, J. Vac. Sci. Technol. A **13**, 1699 (1995).
[7] H. Edwards, V. A. Ukraintsev, R. S. Martin, F. S. Johnson, P. Menz, S. Walsh, S. Ashburn, K. S. Wills, K. Harvey, and M.-C. Chang, J. Appl. Phys. **87**, 1485 (2000).
[8] V. V. Zavyalov, J. S. McMurray, and C. C. Williams, J. Appl. Phys. **85**, 7774 (1999).
[9] P. De Wolf, M. Geva, C. L. Reynolds, T. Hantschel, W. Vandervorst, and R. B. Bylsma, J. Vac. Sci. Technol. A **17**, 1285 (1999).
[10] R. P. Lu, K. L. Kavanagh, St. J. Dixon-Warren, A. Kuhl, A. J. SpringThorpe, E. Griswold, G. Hillier, I. Calder, R. Ares, and R. Streater, J. Vac. Sci. Technol. B **19**, 1662 (2001).
[11] T. Trenkler, P. D. Wolf, W. Vandervorst, and L. Hellemans, J. Vac. Sci. Technol. B **16**, 367 (1998).
[12] T. Trenkler, R. Stephenson, P. Jansen, W. Vandervorst, and L. Hellemans, J. Vac. Sci. Technol. B **18**, 586 (2000).
[13] W. W. Chow, Proc. SPIE **2399**, 445 (1995).
[14] G. L. Pearson, W. T. Read, and W. Shockley, Phys. Rev. **85**, 1055L (1952).
[15] D. Ban, E. H. Sargent, St. J. Dixon-Warren, I. Calder, T. Grevatt, G. Knight, and J. K. White, J. Vac. Sci. Technol. B (in press).
[16] N. W. Ashcroft and N. D. Mermin, *Solid State Physics* (Saunders, Philadelphia, 1976).
[17] C. Kittel, *Introduction to Solid State Physics*, 5th ed. (Wiley, New York, 1976), p. 240.
[18] C. Kittel, *Thermal Physics* (Wiley, New York, 1969), p. 180.
[19] K. Kano, *Semiconductor Devices* (Prentice-Hall, Upper Saddle River, NJ, 1998).

Downloaded 20 Dec 2003 to 128.100.138.68. Redistribution subject to AIP license or copyright, see http://ojps.aip.org/aplo/aplcr.jsp